Thanks are due to E. Gabilli and R. Lotti for their technical assistance.

[1]P. G. Merli and F. Zignani, Radiat. Eff. Lett. **50**, 115 (1980).
[2]R. A. McMahon, M. Ahmed, R. M. Dobson, and J. D. Speight, Electron. Lett. **16**, 295 (1980).
[3]J. M. Mayer and P. T. Clogston, in Proceedings of *Laser Effects in Ion Implanted Semiconductors*, edited by E. Rimini (Istituto Nazionale de Struttura della Materia, Universitá di Catania, Italy, 1978).
[4]G. Masetti and S. Solmi, Solid State and Electron Devices **3**, 65 (1979).
[5]P. K. Madden and S. M. Davidson, Radiat. Eff. **14**, 271 (1972).
[6]R. T. Hodgson, J. E. Baglin, R. Pal, J. M. Neri, and D. A. Hammer, Appl. Phys. Lett. **37**, 187 (1980).
[7]P. G. Merli, Opt. **56**, 205 (1980).

Charge injection over triangular barriers in unipolar semiconductor structures

R. F. Kazarinov and S. Luryi
Bell Laboratories, Murray Hill, New Jersey 07974

(Received 2 February 1981; accepted for publication 5 March 1981)

A theory of unipolar current over triangular barriers in semiconductor structures is developed. Diodes based on such barriers have been recently fabricated by molecular beam epitaxy using either variable-gap or modulation-doped semiconductors. In these diodes the current is due to unipolar injection of electrons. Exact analytic expression for current-voltage characteristics is obtained. Comparison is made with recent experimental data.

PACS numbers: 85.30.Hi, 73.40.Lq, 73.40.Ei

The purpose of this letter is to draw attention to the importance of the phenomenon of charge injection in unipolar semiconductor structures. By charge injection we mean the thermionic emission of electrons over a barrier in a unipolar semiconductor structure when the barrier height is efficiently controlled by an applied voltage. In a certain sense one can say that such a phenomenon is not new. Indeed, in a forward-biased Schottky diode, electrons are injected into the metal from the semiconductor. However, because of the large concentration of electrons in the metal, the injected charge produces no tangible effect on the metal conductivity near the boundary. No charge injection into the semiconductor occurs in a reverse-biased Schottky diode (neglecting a small effect of image-force barrier lowering), and current in this case is limited by thermionic emission over a barrier of fixed height.[1] A similar situation takes place in all-semiconductor analogs of Schottky barriers such as camel diodes[2] and n-n heterojunctions.[3] As before, injection takes place only in the forward-bias regime.

A triangular barrier (TB) structure with finite slopes on both sides possesses a fundamentally new feature: *injection of charge in both directions*, including injection into a high-field region of the semiconductor. Experimental realization of such structures was first reported in Ref. 4 using a variable-gap material (GaAlAs with variable Al content) and more recently in Ref. 5 using a charge sheet built in a homogeneous intrinsic GaAs by modulation doping. In both cases an undoped TB was sandwiched between two n-type layers. The IV characteristics of TB's show exponential growth in both directions and for a sufficiently asymmetical TB rectification was observed.[4,5] In this letter we outline the theory of charge injection over TB, leaving a fuller account for a separate publication.

We restrict our attention to the charge-sheet TB, experimentally realized in Ref. 5 (the theory is readily extended to the case[4] of a variable-gap TB. The structure is shown in Fig. 1(a). It represents a nearly intrinsic i layer of thickness $L\sim(2\text{–}3)\times10^{-5}$ cm sandwiched between two n-type layers of low resistivity. In the process of growth by molecular beam epitaxy (MBE) a p^+-doped layer of thickness $\delta \ll L$ is built into the i region. Acceptors in the p^+-layer are completely ionized forming a charge sheet of surface density Σ which gives rise to a TB with the shoulders L_1 and L_2 and the height approximately equal to $\Sigma L_1 L_2/\epsilon L$, where ϵ is the dielectric permittivity. The typical value of Σ used in Ref. 5 was $\Sigma/q\sim10^{12}\,\text{cm}^{-2}$, and the thickness δ of the charge sheet can be as small as several interatomic distances. The ratio L_1/L_2 can be varied in a controlled fashion from unity to about 10. The charge, field, and potential distributions [Figs. 1(b)–1(d)] are described by the Poisson and the drift-diffusion equations which are adequate on the uphill slope of the barrier and on the lower part of the downhill slope where the electrons are no longer hot. Electrons moving with the saturation velocity on the upper part of the downhill slope give negligible contribution to the field. Eliminating the electron concentration from the two equations one obtains

$$J=\mu\epsilon\frac{\partial}{\partial x}\left[\tfrac{1}{2}E^2+\frac{1}{\beta}\frac{\partial E}{\partial x}\right], \tag{1}$$

where J is the current density, μ the mobility, and $\beta\equiv q/kT$.

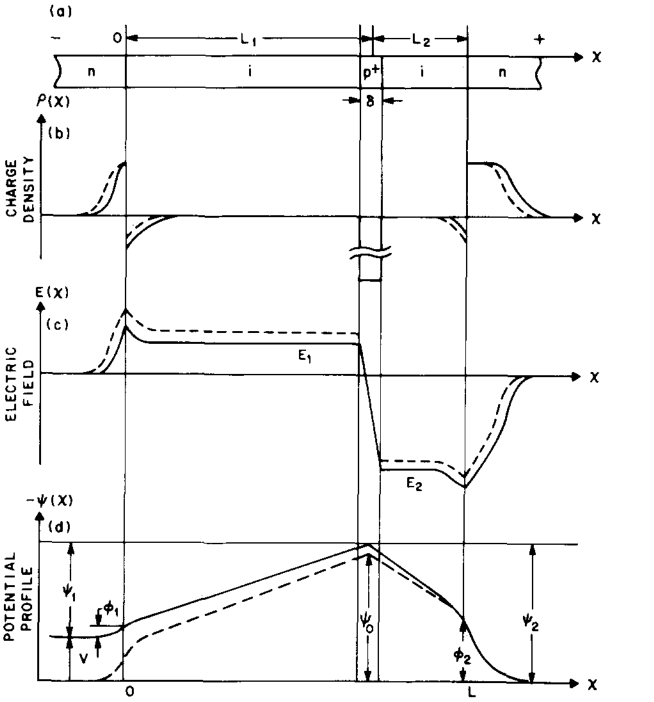

FIG. 1. Schematic diagram of a charge-sheet TB structure (a); charge density (b); electric field (c); and electrostatic potential (d) distributions. Dashed and solid lines correspond, respectively, to the cases of equilibrium and forward bias.

At $x = L_1 \pm \delta/2$ (see Fig. 1), the field E experiences a discontinuity $E_1 - E_2 = \Sigma/\epsilon$ due to the charge sheet of surface density Σ, where $E_1 \equiv E(x = L_1 - \delta/2)$ and $E_2 \equiv E(x = L_1 + \delta/2)$. With $\Sigma/q \sim 10^{12}\ \mathrm{cm}^{-2}$, the discontinuity in the field E is of order 150 kV/cm. When integrated over x, Eq. (1) becomes a nonlinear, first-order differential equation of Riccati type and its solution is of the form[6]

$$E(x) = E_1[\coth(\beta E_1 x + \xi_1) - (J/J_1)\beta E_1 x], \quad 0 \leqslant x < L_1, \qquad (2)$$

where $J_1 \equiv \epsilon\mu\beta E_1^3$. The field $E(x)$ in region $L_1 < x \leqslant L$, where $L \equiv L_1 + L_2$, is obtained from (2) by changing the subscripts $1 \to 2$ and $x \to x - L$. Terms of order $(J/J_1)^2$ were neglected in (2), since $J \ll J_1$ for TB's of practical interest and realistic current densities. Equations relating the constants of integration ξ_i and E_i $(i = 1,2)$ are obtained from the continuity of $E(x)$ and electron concentration at $x = 0, L$:

$$e^{\beta\phi_i} - \beta\phi_i - 1 = (E_i/E_0)^2 \coth^2 \xi_i, \qquad (3)$$

$$e^{\beta\phi_i} = (E_i/E_0)^2 \sinh^{-2} \xi_i, \qquad (4)$$

where $E_0^2 = kTN_d/\epsilon$ with N_d being the donor concentration ($E_0 \sim 60$ kV/cm for $N_d \sim 10^{18}\ \mathrm{cm}^{-3}$), and the ϕ_i's describe the total drop of the electrostatic potential in the n layers on each side of TB, see Fig. 1(d). The electron concentration $n = -(\epsilon/q)\partial E/\partial x$ is found by differentiating Eq. (2). The first term in (2) leads to a barometric formula with the imrefs constant on each side and equal to the corresponding bulk values. The second term describes the imref variation due to current. If the effects of acceleration and heating of electrons on the concentration near $x = L_1$ can be neglected (i.e., when the downhill slope is gentle enough), then the current-voltage characteristic is obtained by simply matching the solutions for $n(x)$ at $x = L_1$. In the opposite case of a steep downhill slope our theory is analogous to the thermionic emission-diffusion theory of Crowell and Sze for Schottky diodes,[1] and the following expression for the current is found:

$$J = A^* T^2 (e^{\beta\psi_1} - e^{\beta\psi_2}), \qquad (5)$$

where A^* is an effective Richardson constant.[1] The potentials ψ_1 and ψ_2 [see Fig. 1(d)] are given by

$$\psi_i = -|E_i|L_i + \frac{kT}{q} \ln\left\{ \frac{2E_i}{E_0}\left[1 + \left(\frac{E_i}{E_0}\right)^2 e^{1 + (E_i/E_0)^2}\right]^{1/2} - \left[\left(\frac{E_i}{E_0}\right)^2 e^{1 + (E_i/E_0)^2}\right]^{1/2}\right\}^2. \qquad (6)$$

Equations (5) and (6) together with the condition $\psi_1 - \psi_2 = V$ and Gauss's law $E_1 - E_2 = \Sigma/\epsilon$ give the diode's I-V curve in a parametrical form in which both I and V are determined in terms of a single dimensionless parameter, say, E_1/E_2.

For sufficiently steep slopes, $E_1^2 > 4kTN_d/\epsilon$, this parameter can be eliminated analytically, and the I-V characteristics reduce to the simple form

$$J = A^* T^2 e^{\beta(\psi_0 - \epsilon V^2/qN_d L^2)}[e^{\beta V l_1} - e^{-\beta V l_2}], \qquad (7)$$

where ψ_0 is the zero-bias barrier height and l_1, l_2 are effective dimensionless lengths of the barrier shoulders

$$l_i = \frac{L_i}{L} + \frac{2\Sigma}{qLN_d}\left(1 - 2\frac{L_i}{L}\right). \qquad (8)$$

The first, "geometric" term in (8) corresponds to a simple model, used in Ref. 5 for a rough interpretation of the experimental data, which neglects the finite space-charge widths near $x = 0$ and $x = L$. This model can be formally obtained from Eqs. (7) and (8) by letting $N_d \to \infty$. However, as stated above, in this limit Eq. (7) is invalid and the exact expressions (5) and (6) should be used. Physically, this means that for $N_d > \epsilon E_i^2/4kT$ the potential due to electrons which diffuse into the i regions becomes important, while the approximation used in (7) corresponds precisely to the neglect of this effect. Thus the geometric model[5] is never a valid approximation.

In Fig. 2 our theory is compared with the experimental I-V curves[5] for the two diodes, A and B, which were of circular geometry with the diameter of 100 μm. The experimental situation for these diodes conforms to the thermionic emission-diffusion theory described by Eqs. (5) and (6). In calculating the I-V characteristics we used the value $A^* \sim 4A$ $\mathrm{cm}^{-2}\ \mathrm{K}^{-2}$, which was assumed in Ref. 5 and the experimental structure parameters except for the donor concentration N_d in the n layers. Our best fit corresponds to the values $N_d \sim 7 \times 10^{18}\ \mathrm{cm}^{-3}$, which is about two times lower than that assumed in Ref. 5. For small currents, outside the experimental range the log I vs V characteristics are linear and the slopes are well described by the ideality factors $1/l_1$, and $1/l_2$, cf. Eq. (8). However, the nonlinearity becomes quite

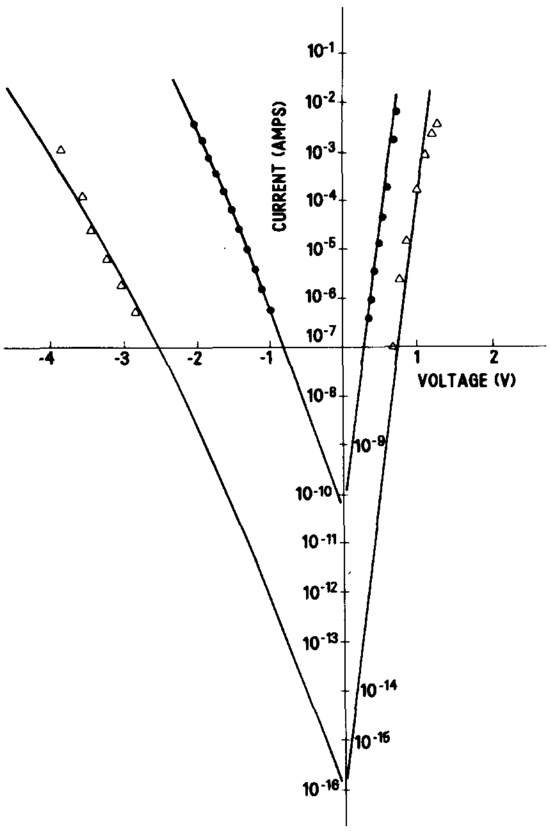

FIG. 2. Theoretical and experimental log I vs V characteristics for two diodes A and B. Experimental data (Ref. 5) are shown in Δ for diode A and in • for B. Solid lines represent our theoretical calculation according to Eqs. (5) and (6). A: $L_1 = 500$ Å; $L_2 = 2000$ Å; $\Sigma/q = 10^{12}\ \mathrm{cm}^{-2}$. B: $L_1 = 250$ Å; $L_2 = 2000$Å; $\Sigma/q = 2\times 10^{12}\ \mathrm{cm}^{-2}$.

appreciable at higher currents. At still higher currents one must take into account the accumulation of carriers drifting with the saturated velocity v_s on the downhill slope of the TB. These carriers screen the applied field which leads to a degradation of the exponential I-V characteristic and its eventual replacement by a linear law. It can be shown that this effect becomes important at current densities $J > J_c$, where $J_c = \epsilon kTv_s/qL_2^2 \sim 10^3\ \mathrm{A/cm}^2$, which is outside the experimental range in Fig. 2.

Discussions with S. M. Sze are gratefully acknowledged.

[1]S. M. Sze, *Physics of Semiconductor Devices* (Wiley, New York, 1969), chap. 8.

[2]J. M. Shannon, Appl. Phys. Lett. **35**, 63 (1979).

[3]A. Chandra and L. F. Eastman, Electron. Lett. **15**, 91 (1979).

[4]C. L. Allyn, A. C. Gossard, and W. Wiegmann, Appl. Phys. Lett. **36**, 373 (1980).

[5]R. J. Malik, T. R. AuCoin, R. L. Ross, K. Board, C. E. C. Wood, and L. F. Eastman, Electron. Lett. **16**, 837 (1980).

[6]E. Kamke, *Differentialgleichungen* (Leipzig, 1959), Vol. I. Strictly speaking, for $\beta E_1 x \sim 1$ the second term in (2) becomes a more complicated function of x, readily obtainable in our theory. However, in such a range of x this term is entirely negligible.